Hindawi
Journal of Nanomaterials
Volume 2023, Article ID 9865132, 1 page
https://doi.org/10.1155/2023/9865132

*Retraction*

# Retracted: Wire Electrical Discharge Machining (WEDM) of Hybrid Composites (Al-Si12/$B_4C$/Fly Ash)

**Journal of Nanomaterials**

Received 11 July 2023; Accepted 11 July 2023; Published 12 July 2023



This article has been retracted by Hindawi following an investigation undertaken by the publisher [1]. This investigation has uncovered evidence of one or more of the following indicators of systematic manipulation of the publication process:

(1) Discrepancies in scope
(2) Discrepancies in the description of the research reported
(3) Discrepancies between the availability of data and the research described
(4) Inappropriate citations
(5) Incoherent, meaningless and/or irrelevant content included in the article
(6) Peer-review manipulation

The presence of these indicators undermines our confidence in the integrity of the article's content and we cannot, therefore, vouch for its reliability. Please note that this notice is intended solely to alert readers that the content of this article is unreliable. We have not investigated whether authors were aware of or involved in the systematic manipulation of the publication process.

Wiley and Hindawi regrets that the usual quality checks did not identify these issues before publication and have since put additional measures in place to safeguard research integrity.

We wish to credit our own Research Integrity and Research Publishing teams and anonymous and named external researchers and research integrity experts for contributing to this investigation.

The corresponding author, as the representative of all authors, has been given the opportunity to register their agreement or disagreement to this retraction. We have kept a record of any response received.

## References

[1] J. Udaya Prakash, P. Sivaprakasam, I. Garip et al., "Wire Electrical Discharge Machining (WEDM) of Hybrid Composites (Al-Si12/$B_4C$/Fly Ash)," *Journal of Nanomaterials*, vol. 2021, Article ID 2503673, 10 pages, 2021.

Hindawi
Journal of Nanomaterials
Volume 2021, Article ID 2503673, 10 pages
https://doi.org/10.1155/2021/2503673

*Research Article*

# Wire Electrical Discharge Machining (WEDM) of Hybrid Composites (Al-Si12/$B_4C$/Fly Ash)

**J. Udaya Prakash ,[1] P. Sivaprakasam ,[2] Ilhan Garip,[3] S. Jebarose Juliyana,[1] G. Elias ,[2] G. Kalusuraman ,[4] and Ilhami Colak[3]**

[1]*Department of Mechanical Engineering, Vel Tech Rangarajan Dr. Sagunthala R&D Institute of Science and Technology, Chennai, India*
[2]*Department of Mechanical Engineering, College of Electrical and Mechanical Engineering, Addis Ababa Science and Technology University, Addis Ababa, Ethiopia*
[3]*Department of Electrical and Electronics Engineering, Nisantasi University, Istanbul, Turkey*
[4]*Department of Agricultural Engineering, Kalasalingam Academy of Research and Education, Krishnankoil, Tamil Nadu, India*

Correspondence should be addressed to P. Sivaprakasam; shiva@aastu.edu.et and G. Elias; elias.gmichael@aastu.edu.et

Received 24 October 2021; Revised 21 November 2021; Accepted 24 November 2021; Published 13 December 2021

Academic Editor: Karthikeyan Sathasivam



The present study looks into the effect of WEDM process parameters on the material removal rate (MRR) and surface roughness (SR) responses when machining hybrid composites (Al-Si12/boron carbide/fly ash) using the Taguchi technique. Fly ash and boron carbide ($B_4C$) particles were used for reinforcement (3%, 6%, and 9% by weight), and aluminium alloy (Al-Si12) was used as a matrix material. ANOVA was used to find out the importance of machining factors that affect the quality features of the WEDM process, as well as the relative role of input parameters in determining the WEDM process' responses. The greatest impact on the response is finalised by the signal-to-noise (S/N) ratio response analysis. However, as a last step, a confirmation experiment with the best combination was carried out to predict and validate the accuracy of the observed values. As the pulse on time and reinforcement increases, MRR also increases. As the gap voltage, wire feed, and pulse off time decrease, it increases. SR is increased by increasing the gap voltage, pulse on time, and pulse off time, wire feed, and reinforcement. The maximum MRR of 38.01 $mm^3$/min and the minimum SR of 3.24 $\mu$m were obtained using optimal machining conditions.



## 1. Introduction

Composite materials are produced by combining two or additional materials in order that they mechanically function as one single entity. A hard phase may be incorporated into a soft phase or vice versa. The hard phase functions as a reinforcing agent in most composite materials, increasing elastic modulus, while the soft phase serves as a matrix. The advantage of using composites is that they can achieve proved to be beneficial and may end up in a variety of service advantages such as enhanced strength, significantly reduced weight, enhanced wear resistance, and high elastic modulus [1]. The foremost benefit of composites is the potential of their mechanical and physical properties to be aimed at meeting unique design standards. Particulate-reinforced metal matrix composites (MMCs) possess high stiffness but low strength, as well as outstanding fabricability, less cost, and homogeneity. The traditional reinforcement materials for AMCs are SiC and $Al_2O_3$. Because $B_4C$ powder is more expensive than SiC and $Al_2O_3$, there have been few studies on boron carbide-reinforced MMCs. There is a growing demand for composites with low-density, low-cost reinforcement particles. Fly ash is a lightweight, lower cost material that is widely available [2]. As a result, fly ash-reinforced composites are liable to break through the price barrier for the widespread use in automobiles. The insertion of fly ash particles increases the hardness, rigidity, impact resistance, and damping qualities of

Al alloys while decreasing their density. Al-fly ash composites offer potential uses in the automobile, turbocharged engine, and electrical industries as cloaks, shells, shafts, coverings, plates, manifolds, valve encompasses, brake discs, and other engine parts.

Metal matrix composites have the potential to outperform traditional metals in terms of efficiency, dependability, and mechanical performance. When compared to continuously reinforced competitors, particle-reinforced MMCs are particularly appealing since they display isotropic characteristics [3]. Particulate-reinforced MMCs have the added benefit of being malleable and workable. The fundamental disadvantage of MMCs is that they have poor mechanical properties and fracture toughness in comparison to their matrix material. Stir casting is the most cost-effective of all MMC industrial uses. It entails mechanically mixing the reinforcing particles into a liquid metal bath and directly moving the mix to a mould [4]. The most important aspect of this technique is achieving adequate wetting between both the particle reinforcements and the molten metal. Because of the contact between flocculated ceramic particles and the solid-liquid interface, it is difficult to achieve homogeneous reinforcement distribution in these cast composite materials. This method may be used to create very big components. A considerable number of engineers and scientists are now researching the synthesis, characterisation, and performance assessment of DRMMCs in universities and research institutes. DRMMCs have found applications in aircraft, automotive, and a variety of other scientific and commercial fields.

Clearly, the liquid metallurgical process is the most economically feasible of all MMC manufacturing techniques. The stir casting process, often known as the vortex technique, is the most basic and widely used technique. In general, ceramic particles with sizes ranging from 5 to 100 $\mu$m may be included in a wide spectrum of molten aluminium alloys. Furthermore, this technique enables the fabrication of very massive components. The microstructure and hardness of composites are influenced by the stirring speed and duration. At 600 rpm and 10 minutes of stirring, uniform particle dispersion and higher hardness values were attained [5].

In the aluminium 2024 matrix, larger $B_4C$ particles 71 $\mu$m were typically homogenous, but smaller particles (29 $\mu$m) caused clumping, segregation, and high porosity. The density of the composites dropped as the volume percentage of the particles increased and the particle size decreased; the porosity and hardness of the composites increased as the content increase and the particle size decreased [6]. The inclusion of $B_4C$ particles significantly enhanced the abrasive wear characteristics of the 2024 aluminium alloy. According to microstructural analysis, the $B_4C$ particles were uniformly dispersed. In the stir casting process, the particle dispersion of $B_4C$ enhanced by the inclusion of 250°C warmed particles, which resulted in a homogeneous grain structure in the composite [7]. Si is crucial in the development of a barrier layer, which can restrict $B_4C$ breakdown and increase $B_4C$ stability in the aluminium melt.

Magnesium plays a critical role in composite fabrication by removing $O_2$ first from dispersed surfaces, reducing the gaseous layer, and enhancing wetting. The first 1 wt% Mg addition results in a very dramatic drop in surface tension. However, as Mg concentration increases, the reduction becomes extremely minor. Magnesium and aluminium mixtures appear to have a synergistic impact on wetting. The particle dispersion of fly ash is consistent and strong interfacial bonding exists between the matrix and the fly ash particles.

Fly ash is abundant as a waste by-product of coal-fired power plants' combustion processes. It is used in aluminium castings to reduce energy capacity, material content, price, and mass of components, as well as enhance wear resistance. The matrix and fly ash particles have strong interfacial bonding. The hardness rises as the fly ash concentration increases. The composite's mechanical characteristics are improved, but its ductility is decreased when the weight of the fly ash particles increases. The micrographs of the samples indicate that the fly ash particles are distributed uniformly [8].

ANOVA is used to assess the significance of machining factors on MRR and SR. S/N ratio analysis is used to find the optimal machining settings. The effects of machining parameters on SR in WEDM finish cuts and discovered that SR may be reduced by reducing both pulse on time and current. Different methods are used for improving the performance of wire electro-discharge machining by utilising pulse train features. The analysis indicates that the Taguchi technique is better suited to solving the stated problem with fewer experiments than a complete factorial design [9].

Nowadays, MMCs are widely used in industries; their higher hardness and reinforcement make conventional machining challenging, especially when complicated forms and precise components are required. Because it is easier to cut and complex forms, WEDM is the ideal choice for machining composites. The manufacturer's machining parameters database is useful, but it is inadequate. Furthermore, it is traditional machining and does not lead to optimal and cost-effective machine use. As a result, optimizing the WEDM process parameters is unavoidable [10].

Traditional technology used to process tough composite materials produces tool wear [11]. Although in other sophisticated nonconventional machining, the equipment is expensive and the work piece height is limited. The machining parameters sometimes fail to satisfy the criteria and provide suitable guidance to production engineers. As a result, a suitable selection of WEDM process parameters is required.

WEDM provides enormous potential for diversity of application and complicated physical processes in unconventional machining techniques. Intricate and complicated forms can be machined. WEDM removes material via spark erosion all across the wire electrode and work piece. Electromachining can shape and treat electrically conductive materials. Its machining, however, varies from that of typical metallic materials. It is common knowledge that increasing the hardness of the work material during typical machining processes results in a decrease in economic cutting speed [12].

Table 1: Aluminium alloy (Al-Si12) chemical composition.

| Constituent | Fe | Cu | Si | Mg | Ni | Ti | Zn | Mn | Al |
|---|---|---|---|---|---|---|---|---|---|
| Weight % | 0.52 | 0.013 | 11.48 | 0.02 | 0.01 | 0.02 | 0.01 | 0.01 | Remainder |

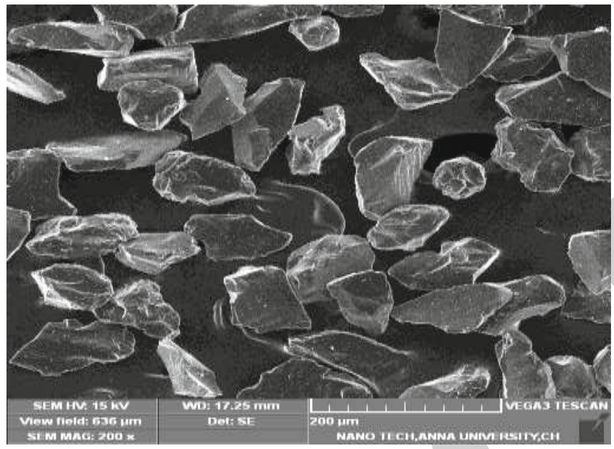


Figure 1: SEM image of boron carbide particles.

Table 2: Fly ash chemical composition.

| Constituent | Si | O | Al | Fe | Ti | Ca | K | LOI |
|---|---|---|---|---|---|---|---|---|
| Weight % | 26.43 | 38.88 | 16.73 | 3.82 | 1.42 | 0.5 | 0.99 | Remainder |

Tool materials that are extremely hard and strong to cut materials that is no longer available. Traditional techniques of producing complicated forms in such materials are still more challenging; additionally, it requires greater finish, low tolerance values, larger production rates, complex shapes, and so forth. To address all of these challenges, advanced machining techniques, also known as nontraditional machining processes, have been created. According to the research, using a magnetic field to enhance micro-EDM has a larger MRR than using one without a magnetic field [13, 14]. Adding graphite nanopowder to a dielectric fluid while utilising micro-WEDM can greatly improve the surface finish [15].

The ever-increasing need in the car industry for low weight, fuel efficiency, and comfort has resulted in the development of sophisticated lightweight composite materials with optimal design. The use of aluminium matrix composites in vehicles has the potential to improve fuel efficiency. Abrasion resistance is enhanced by the presence of hard boron carbide in the Al matrix. Similarly, the inclusion of fly ash in an Al matrix might result in a low-weight composite. Lightweight abrasion-resistant composites for wear resistance applications may be created by combining boron carbide with fly ash [16]. Hard boron carbide in the Al alloy matrix limits machinability, and standard tools are ineffective. The motivation for selecting the reinforcing mass fractions and sizes is based on the ease with which the particles may be incorporated into the matrix and castability. One of the potential technologies for efficient machining of hard particle-reinforced metal matrix composites is WEDM. The most popular Al-cast alloy used in the automobile industry is Al-Si12. As a result, an attempt was made to investigate the possibility of producing Al-Si12-reinforced with fly ash and boron carbide. The scope also includes measuring density, hardness, and WEDM machinability investigations.

## 2. Materials and Methods

*2.1. Aluminium Alloy.* Aluminium alloy (Al-Si12) has good corrosion resistance. It has the ability to be cast into thinner and more complex pieces than other form of casting alloy. Table 1 shows the composition of Al-Si12.

*2.2. Boron Carbide.* Boron carbide ($B_4C$) particles with a diameter of 63 $\mu$m were employed as one of the reinforcing materials in this investigation. $B_4C$ has a number of attractive characteristics, including widespread application as cermets and armour materials. Figure 1: SEM image depicting the shape of boron carbide particles.

*2.3. Fly Ash.* Another reinforcement material employed in this investigation was fly ash (12 $\mu$m) particles. The inclusion of fly ash particles into aluminium alloys lowers their density and enhances their mechanical properties. Fly ash particles are cheap and low-density waste by products of thermal power plants that are available in huge quantities. The low thermal conductance, high electrical resistance, and low density of the material may be advantageous in the creation of lightweight insulating composites. Chemical analysis was used to determine the composition of fly ash. Table 2 shows the chemical composition, and Figure 2 shows the SEM image of fly ash.

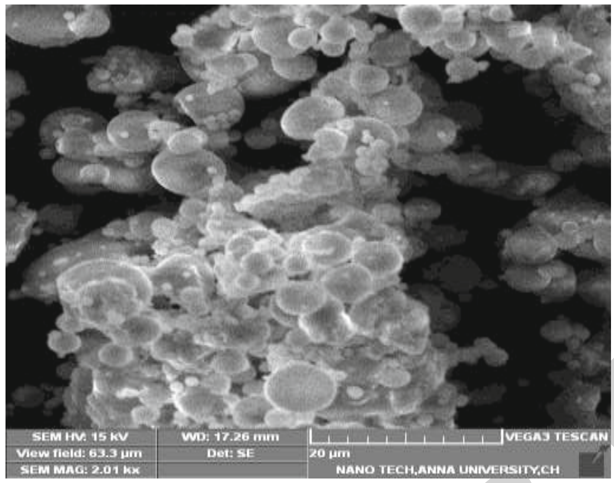


Figure 2: SEM image of fly ash particles.

(a) (b)

Figure 3: (a) Stir casting setup (b) with furnace.

Figure 4: Photograph of wire EDM machine.

Table 3: WEDM input parameters and their levels.

| Level | Input parameters | | | | |
|---|---|---|---|---|---|
| | Gap voltage (V) | Pulse on time ($\mu$s) | Pulse off time ($\mu$s) | Wire feed (m/min) | Reinforcement (%) |
| 1 | 30 | 2 | 2 | 4 | 3 |
| 2 | 50 | 6 | 6 | 6 | 6 |
| 3 | 70 | 10 | 10 | 8 | 9 |

*2.4. Stir Casting.* The composites were made using a stir casting process. This is a liquid-state composite production method. Stir casting is the modest and most useful liquid state manufacturing process. Figure 3 shows the stir casting setup for composites.

*2.4.1. Fabrication of Hybrid Composites.* Al-Si12 (aluminium alloy) ingots were liquefied in an electric furnace using a graphite crucible. The temperature was progressively increased to 850°C. A degasser (hexachloroethane) was used to degass the melt at 800°C. The fluid metal was stirred, and

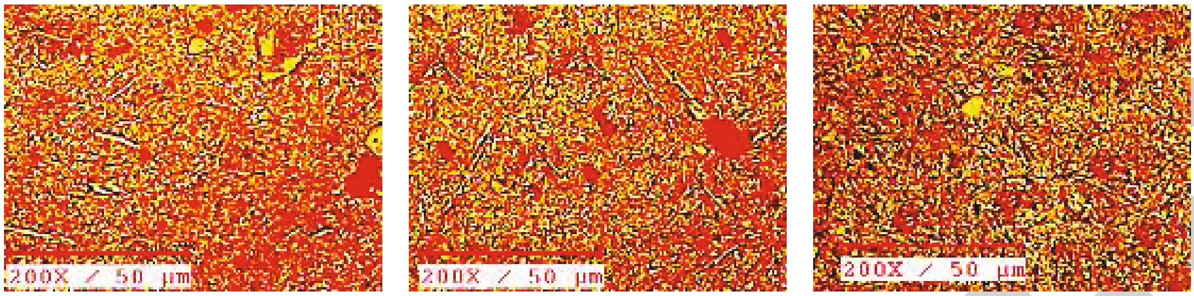


(a) Al-Si12+3% $B_4C$ and fly ash (b) Al-Si12+6% $B_4C$ and fly ash (c) Al-Si12+9% $B_4C$ and fly ash

Figure 5: (a–c) Micrographs of fabricated composites.

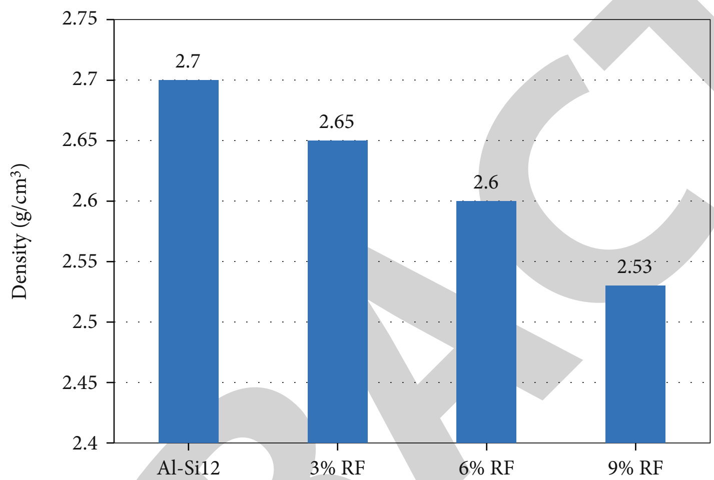


Figure 6: Effects of boron carbide and fly ash on composite density.

then, particles of $B_4C$ and fly ash were added at 250°C. For 10 minutes, the slurry was mixed at 600 rpm [17]. In the molten metal, potassium hexaflurotitanate (1% wt) was introduced. The inclusion of titanium into the Al/$B_4C$ composite casting results in the formation of a reactive zone on the interfaces, which improves water solubility, interfacial interaction, and the elimination of the oxide deposition on the metal substrate. The tiny quantity of these additions had no discernible effect on the matrix alloys' properties (1 wt. percent). Boron carbide was added in quantities of 1.5, 3, and 4.5 percent by weight, respectively. The fly ash was delivered in weight fractions of 1.5, 3, and 4.5 percent. The liquid metal was poured into cast iron moulds that had been preheated to 650°C and then allowed to solidify.

*2.5. Working Principle.* In wire EDM, a nozzle injects deionized water (dielectric) into the machining area. A pulsed DC supply is used to power the electrodes (wire and work piece). The heat generated by sparking causes the work piece and wire material to melt, and a portion of the material may even vaporise, as in traditional EDM. A positioning system maintains a constant separation between the tool (wire) and the work piece. This method cuts complex curves, especially in materials that are tough to process. This approach provides a high level of precision as well as a good surface finish [18]. The experimental set up used for WEDM of composites shown in Figure 4.

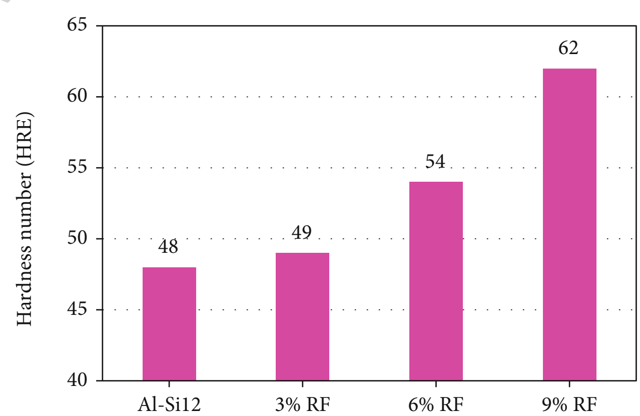


Figure 7: Effects of boron carbide and fly ash on composites (HRE).

*2.6. Design of Experiments.* The design of experiments (DoE) method is used to identify factors that influence a product. DoE reduces the number of experimental runs required to collect the necessary data significantly. DoE utilizing the Taguchi method has turned out to be a far more useful tool for practicing engineers and scientists.

Table 4: Experimental results of MRR and SR (Al-Si12/$B_4C$/fly ash).

| Ex. no | *A* Gap voltage (V) | *B* Pulse on time ($\mu$s) | *C* Pulse off time ($\mu$s) | *D* Wire feed (m/min) | *E* Reinforcement (wt%) | MRR ($mm^3$/min) | SR ($\mu$m) | S/N for MRR | S/N for SR |
|---|---|---|---|---|---|---|---|---|---|
| 1 | 30 | 2 | 2 | 4 | 3 | 25.514 | 3.38 | 28.14 | -10.58 |
| 2 | 30 | 2 | 6 | 6 | 6 | 21.423 | 3.06 | 26.62 | -9.71 |
| 3 | 30 | 2 | 10 | 8 | 9 | 17.262 | 3.57 | 24.74 | -11.05 |
| 4 | 30 | 6 | 2 | 6 | 9 | 33.112 | 3.97 | 30.40 | -11.98 |
| 5 | 30 | 6 | 6 | 8 | 3 | 26.104 | 3.3 | 28.33 | -10.37 |
| 6 | 30 | 6 | 10 | 4 | 6 | 25.705 | 3.51 | 28.20 | -10.91 |
| 7 | 30 | 10 | 2 | 8 | 6 | 39.086 | 3.98 | 31.84 | -12.00 |
| 8 | 30 | 10 | 6 | 4 | 9 | 31.122 | 3.74 | 29.86 | -11.46 |
| 9 | 30 | 10 | 10 | 6 | 3 | 25.689 | 3.59 | 28.19 | -11.10 |
| 10 | 50 | 2 | 2 | 4 | 3 | 21.058 | 3.3 | 26.47 | -10.37 |
| 11 | 50 | 2 | 6 | 6 | 6 | 16.457 | 3.43 | 24.33 | -10.71 |
| 12 | 50 | 2 | 10 | 8 | 9 | 13.54 | 4.02 | 22.63 | -12.08 |
| 13 | 50 | 6 | 2 | 6 | 9 | 26.772 | 3.4 | 28.55 | -10.63 |
| 14 | 50 | 6 | 6 | 8 | 3 | 20.165 | 3.66 | 26.09 | -11.27 |
| 15 | 50 | 6 | 10 | 4 | 6 | 19.543 | 3.07 | 25.82 | -9.74 |
| 16 | 50 | 10 | 2 | 8 | 6 | 31.742 | 3.45 | 30.03 | -10.76 |
| 17 | 50 | 10 | 6 | 4 | 9 | 22.764 | 3.57 | 27.15 | -11.05 |
| 18 | 50 | 10 | 10 | 6 | 3 | 20.549 | 3.59 | 26.26 | -11.10 |
| 19 | 70 | 2 | 2 | 4 | 3 | 12.321 | 3.24 | 21.81 | -10.21 |
| 20 | 70 | 2 | 6 | 6 | 6 | 9.995 | 3.86 | 20.00 | -11.73 |
| 21 | 70 | 2 | 10 | 8 | 9 | 8.378 | 4.21 | 18.46 | -12.49 |
| 22 | 70 | 6 | 2 | 6 | 9 | 16.365 | 3.97 | 24.28 | -11.98 |
| 23 | 70 | 6 | 6 | 8 | 3 | 12.339 | 3.4 | 21.83 | -10.63 |
| 24 | 70 | 6 | 10 | 4 | 6 | 11.429 | 3.45 | 21.16 | -10.76 |
| 25 | 70 | 10 | 2 | 8 | 6 | 18.475 | 3.49 | 25.33 | -10.86 |
| 26 | 70 | 10 | 6 | 4 | 9 | 14.489 | 3.65 | 23.22 | -11.25 |
| 27 | 70 | 10 | 10 | 6 | 3 | 12.719 | 3.29 | 22.09 | -10.34 |

*2.6.1. Taguchi Method.* The Taguchi method is used in product design and quality improvement. It presents the design engineer with a quick and easy way to determine near-optimal design parameters. To analyze as many variables as possible with a small number of experiments, the Taguchi technique employs OA from the DoE theory. Selecting the most relevant OA and assigning the parameters and their interactions to the proper columns are the first step in designing an experiment. The Taguchi approach maximizes the S/N ratio, a statistical measure of performance that is used to find the best parametric combination. The three most common signal-to-noise ratios are the lower the better, the higher the better, and nominal-the-best. The Taguchi experimental design, which heavily relies on orthogonal arrays, is a powerful method for increasing process/product quality with a small number of trials. The method can improve performance characteristics by determining the appropriate parameter settings and lowering the system's susceptibility to sources of variation. For high productivity and low cost components, manufacturers optimise process parameters. The Taguchi approach is aimed at improving a specific response characteristic. Table 3 shows the machining input parameters and their levels.

## 3. Results and Discussion

*3.1. Microstructure.* Metallographic analyses are an important-to-investigative technique as well as a potent quality control tool. Samples were cut from each composite and finely polished to achieve a mirror-like surface. The fundamental goal of microstructural analysis is to ensure that reinforcement particles are dispersed uniformly throughout the matrix. The optical microscope examines the composite specimens [19]. Figures 5(a)–5(c) show the optical micrographs demonstrating the matrix's homogenous dispersion of reinforcing particles (boron carbide and fly ash).

Figure 5(a) depicts the distribution of the 3 percent hybrid ($B_4C$ and fly ash) composite. The eutectic elements of the Al-Si alloy Al-Si12 are lengthy, acicular, script-like, and unaltered. The micrographs of hybrid metal matrix composites of Al-Si12 alloys with 6% addition of hybrid ($B_4C$ and fly ash) composites are shown in Figure 5(b). In

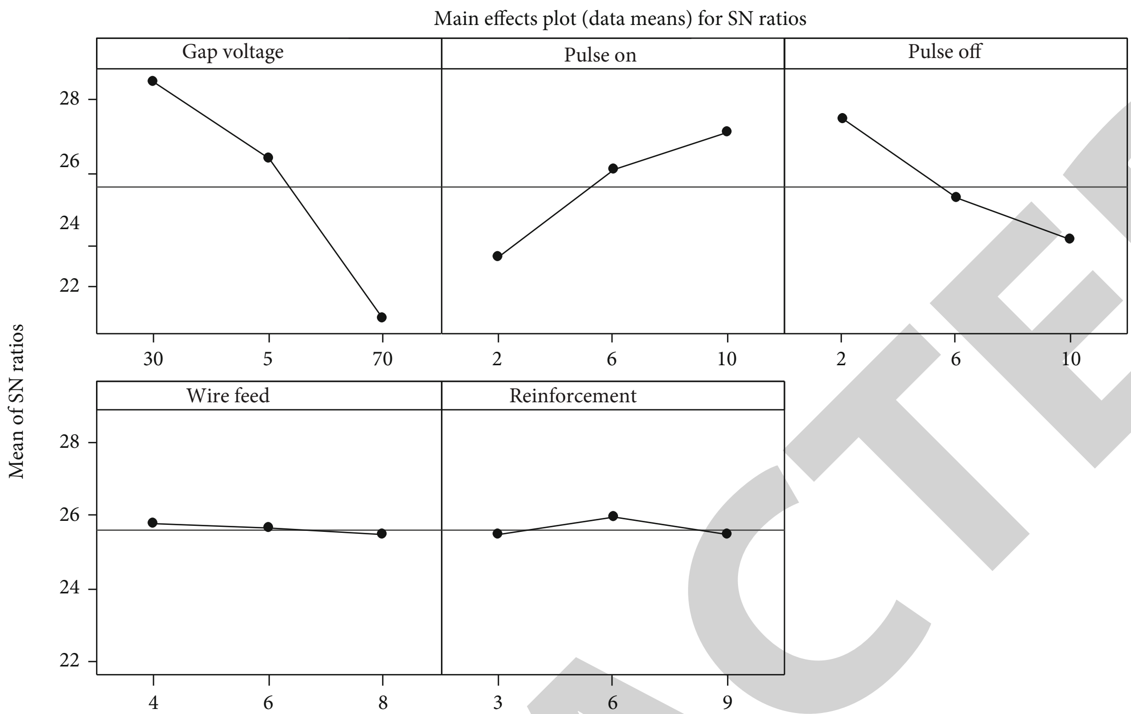


Figure 8: MRR (Al-Si12/boron carbide/fly ash) response graphs.

Al-Si12, the Al-Si eutectics are big, script-like, and have sharp angles. On the other hand, composite dispersion is even, and Al-Si is finer. Figure 5(c) depicts micrographs of 9 percent hybrid ($B_4C$ and fly ash) aluminium matrix composites. The distribution of Al-Si12 alloys is uniform. Due to the increased silicon content in Al-Si12 alloys, this distinctive homogeneous distribution tendency is preserved.

*3.2. Density.* The density is a physical attribute that replicates the properties of composites. It is determined experimentally by utilising displacement techniques [20] and an ASTM D 792-66 test procedure. The standard formula that is used to calculate the density is given in Equation (1).

$$\text{Density} = \frac{\text{Mass}}{\text{Volume}}. \quad (1)$$

The mass is determined using an electronic weighing system with a precision of 0.001 grams. The volume of specimens was determined by a graduated cylinder from the displacement of water. Figure 6 shows the effect of reinforcement (RF) on the density of the composites. The densities of all the composites are observed to be lower than the parent metal. It is because the densities of reinforcements are lower than the matrix material.

*3.3. Hardness.* Resistance to scratching, indentation, distortion, and abrasion are all examples of hardness. The Rockwell test compares the depth of indenter penetration under a huge load to the depth of preload penetration to assess hardness. There are many scales that employ various loads or indenters. The samples were initially polished, and at least five different measurements were taken in each sample at random and averaged to determine the specimen's exact hardness [21]. Figure 7 shows the effect of reinforcement on the hardness of the composites.

Table 5: MRR (Al-Si12/boron carbide/fly ash) response table.

| Level | Gap voltage | Pulse on time | Pulse off time | Wire feed | Reinforcement |
|---|---|---|---|---|---|
| 1 | 28.48 | 23.69 | 27.43 | 25.76 | 25.47 |
| 2 | 26.37 | 26.07 | 25.27 | 25.63 | 25.93 |
| 3 | 22.02 | 27.11 | 24.17 | 25.48 | 25.48 |
| Delta | 6.46 | 3.42 | 3.26 | 0.28 | 0.46 |
| Rank | 1 | 2 | 3 | 5 | 4 |

Table 6: MRR (Al-Si12/boron carbide/fly ash) ANOVA.

| Source | DOF | Sum of squares | Mean sum of squares | $F$ | Contribution (%) |
|---|---|---|---|---|---|
| $A$ | 2 | 195.37 | 97.69 | 849.43 | 64.60% |
| $B$ | 2 | 55.37 | 27.69 | 64.09 | 18.31% |
| $C$ | 2 | 49.38 | 24.69 | 57.15 | 16.33% |
| Error (pooled) | 20 | 2.3 | 0.115 | | 0.76% |
| Total | 26 | 302.42 | | | 100% |

The hardness of composites was found to be greater than that of the base alloy. The addition of hard particles ($B_4C$ and fly ash) increases the hardness of composites by increasing their resistance to plastic deformation. When reinforcement particles are added to composites, the surface area of the reinforcement is raised and the grain size of the matrix is reduced. The presence of such strong reinforcing particles

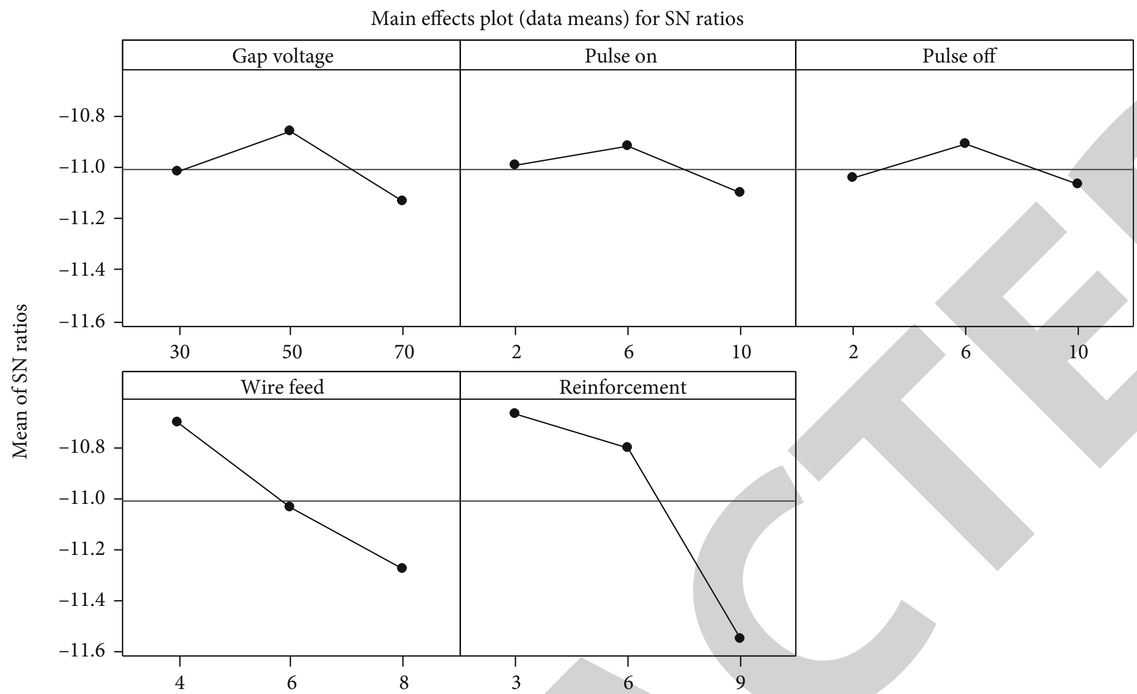


Figure 9: Response graphs for SR (Al-Si12/boron carbide/fly ash).



on the surface prevents the material from deforming due to plastic deformation. By raising the weight percentage of reinforcement, the strength of the grain boundaries is enhanced to its extreme level, and the displacement of atoms is reduced, resulting in higher matrix strength and composite hardness.

*3.4. WEDM of Hybrid Composites.* The experimental results on WEDM of hybrid Al-Si12/$B_4C$/fly ash AMCs are presented in this section. The MRR and SR were the focus of the analysis [22]. An S/N ratio analysis was utilized to select optimal process parameters.

*3.4.1. Experimental Results.* The purpose of the WEDM experiments was to test the influence of process factors on output responses. Experimental results for MRR, SR, and S/N ratios are presented in Table 4.

*3.4.2. Analysis of MRR.* The S/N ratio of each variable at various values was calculated using experimental data. The special effects of S/N data process factors were displayed. Analyzing the response graphs and ANOVA tables yields the most favourable values of process variables in terms of the average performance parameters. The effect of process parameters on MRR was investigated using $L_{27}$ OA experiments. As seen in Figure 8, MRR increases with increasing reinforcement and pulse on time.

It decreases as the gap voltage, wire feed, and pulse off time increases. The discharge energy rises as the pulse lengthens, resulting in a quicker rate of material removal. The frequency of discharges during a given period increases as the pulse off time decreases, resulting in a greater MRR. The average discharge gap widens as the gap voltage rises, resulting in a decreased MRR [23, 24]. Wire feed and reinforcement have no major effects on MRR. MRR is, likewise, evidently lowest at the low level of pulse on time and highest at the low level of pulse off time.

*3.4.3. Optimal Levels for MRR.* Table 5 shows the response table S/N statistics for each factor level. The significance of each element in the response is indicated by the ranks. As shown by the rankings and delta values, gap voltage has the most effect on MRR, followed by other process variables. Figure 8 depicts the maximum MRR in the WEDM process for the level 1 of gap voltage, level 3 of pulse on time, level 1 of pulse off time, and wire feed, and the level 2 of reinforcement. $F_{0.05,2,20} = 3.49$ as can be shown in ANOVA Table 6, gap voltage, pulse on time, and pulse off time are all significant. The error term included the percentage reinforcement, wire feed, and the interactions of gap voltage with other process variables.

*3.4.4. MRR-Confirmation Experiments.* The optimal parameters are employed in the confirmation experiments as well as in estimating the MRR. The outcomes of the experiments are examined in order to determine the optimal parameters. The factors at level $A_1, B_3, C_1, D_1$, and $E_2$ are shown in Figure 8 and response Table 5. The optimal parameters for getting maximum MRR are 30 V gap voltage, 10 $\mu$s pulse on time, 2 $\mu$s pulse off time, 4 m/min wire feed, and 6% reinforcement. MRR is expected to be 36.12 $mm^3$/min, whereas the experimental measurement is 38.01 $mm^3$/min.

*3.4.5. Analysis of SR.* Experiments using $L_{27}$ OA were carried out to examine the influence of process factors on surface roughness. Table 4 displays the experimental results of SR.

Table 7: Response table for SR (Al-Si12/boron carbide/fly ash).

| Level | Gap voltage | Pulse on time | Pulse off time | Wire feed | Reinforcement |
|---|---|---|---|---|---|
| 1 | -11.02 | -10.99 | -11.04 | -10.70 | -10.66 |
| 2 | -10.86 | -10.92 | -10.91 | -11.03 | -10.80 |
| 3 | -11.14 | -11.10 | -11.06 | -11.28 | -11.55 |
| Delta | 0.28 | 0.18 | 0.15 | 0.58 | 0.89 |
| Rank | 3 | 4 | 5 | 2 | 1 |

Table 8: ANOVA for SR (Al-Si12/boron carbide/fly ash).

| Source | DOF | Sum of squares | Mean sum of squares | $F$ | Contribution (%) |
|---|---|---|---|---|---|
| $D$ | 2 | 1.502 | 0.751 | 5.48 | 11.60% |
| $E$ | 2 | 4.123 | 2.062 | 15.05 | 31.85% |
| $AB$ | 4 | 2.682 | 0.671 | 4.89 | 20.72% |
| $AC$ | 4 | 1.787 | 0.447 | 3.26 | 13.81% |
| $AE$ | 4 | 1.481 | 0.370 | 2.70 | 11.44% |
| Error (pooled) | 10 | 1.370 | 0.137 | | 10.58% |
| Total | 26 | 12.945 | | | 100% |

For S/N data, Figure 9 illustrates the SR for all parameters at levels 1, 2, and 3. The SR is increased by increasing the gap voltage, pulse on time, pulse off time, wire feed, and reinforcing. As the pulse lengthens, the discharge energy (DE) increases, and a larger DE produces a larger crater, resulting in higher work piece surface roughness. The frequency of discharges decreases as the pulse off time increases, resulting in an improved surface finish due to stable machining.

*3.4.6. Selection of Optimal Levels for SR.* The S/N data of each factor at each level is shown in Table 7. The outcomes of the experiments are examined to determine the best parameters. Figure 9 shows that in the WEDM process, the second level of gap voltage, pulse on time, and pulse off time, first level of wire feed, and first level of reinforcement offer the lowest SR [25]. ANOVA was used to investigate the importance of the process factors in relation to SR. $F_{0\cdot 05,2,10} = 4.10$ and $F_{0.05,4,10} = 3.48$ are the $F$ values from the table at the 5% significance level. So, according to ANOVA Table 8, wire feed and reinforcement and the interaction of gap voltage with pulse on time are the effective parameters. The error term was made up of the gap voltage, pulse on time, pulse off time, and the interactions of gap voltage with wire feed.

*3.4.7. Confirmation Experiments-SR.* The optimal parameters are employed in the confirmation tests as well as in estimating the SR. The outcomes of the experiments are examined in order to determine the optimal parameters. The factors at level $A_2, B_2, C_2, D_1$, and $E_1$ are shown in Figure 9 and Table 7. The following settings produce the lowest SR: gap voltage of 50 V, pulse on time of 6 $\mu$s, pulse off time of 6 $\mu$s, wire feed of 4 m/min, and reinforcement of 3%. The predicted SR is 3.15 $\mu$m, while the experimental SR is 3.24 $\mu$m.

## 4. Conclusions

In this study, the effects of control parameters on material removal rate and surface roughness in WEDM of Al-Si12/$B_4C$/fly ash composites were investigated, with the following findings:

(1) The optimal factors and their levels for the maximum MRR and minimal Ra were defined. $A_1, B_3, C_1, D_1$, and $E_2$ (gap voltage 30 V, pulse on time: 10 $\mu$s and pulse off time: 2 $\mu$s, wire feed: 4 m/min, and reinforcement percentage 6%) and $A_2$, $B_2$, $C_2$, $D_1$, and $E_1$ (gap voltage 50 V, pulse on time: 6 $\mu$s, pulse off time 6 $\mu$s: wire speed: 4 m/min, and reinforcement percentage 3%)

(2) The most significant parameter on MRR was gap voltage (64.60%), followed by pulse on time (18.31%). The MRR increased as the pulse on time increased

(3) The reinforcement percentage is the most significant factor in surface roughness, with a contribution of 31.85%, whereas the other machining parameters have no effect. Furthermore, the Ra increased as the wire feed and pulse on time values increased; the lowest Ra values were recorded at a pulse off time of 6 $\mu$s

(4) The predicted MRR was determined to be 36.12 $mm^3$/min, compared to 38.01 $mm^3$/min in the experimental measurements

(5) In the WEDM of the Al-Si12/$B_4C$/fly ash composite in the interval of the specified machining circumstances, the predicted surface roughness is 3.15 $\mu$m, whereas the experimental measurement is 3.24 $\mu$m

(6) The Taguchi approach could be effectively utilized for optimizing machining parameters in WEDM operations

## Data Availability

The data used to support the findings of this study are included within the article.

## Conflicts of Interest

The authors declare that they have no conflicts of interest regarding the publication of this paper.

## References


[1] M. K. Surappa, "Aluminium matrix composites: challenges and opportunities," *Sadhana*, vol. 28, Parts 1 & 2, pp. 319–334, 2003.

[2] M. K. Surappa, "Microstructure evolution during solidification of DRMMCs (discontinuously reinforced metal matrix

composites): state of art," *Journal of Materials Processing Technology*, vol. 63, no. 1-3, pp. 325–333, 1997.

[3] M. K. Surappa and P. K. Rohatgi, "Preparation and properties of cast aluminium-ceramic particle composites," *Journal of Materials Science*, vol. 16, no. 4, pp. 983–993, 1981.

[4] T. S. Srivatsan, I. A. Ibrahim, F. A. Mohamed, and E. J. Lavernia, "Processing techniques for particulate-reinforced metal aluminum matrix composites," *Journal of Materials Science*, vol. 26, no. 22, pp. 5965–5978, 1991.

[5] S. BalasivanandhaPrabu, L. Karunamoorthy, S. Kathiresan, and B. Mohan, "Influence of stirring speed and stirring time on distribution of particles in cast metal matrix composite," *Journal of Materials Processing Technology*, vol. 171, no. 2, pp. 268–273, 2006.

[6] H. Singh and R. Garg, "Effects of process parameters on material removal rate in WEDM," *Journal of Achievements in Materials and Manufacturing Engineering*, vol. 32, no. 1, pp. 70–74, 2009.

[7] V. K. Saini, Z. A. Khan, and A. N. Siddiquee, "Optimization of wire electric discharge machining of composite material ($Al6061/SiC_p$) using Taguchi method," *International Journal of Mechanical and Production Engineering*, vol. 2, no. 1, pp. 61–64, 2013.

[8] H. C. Anilkumar, H. S. Hebbar, and K. S. Ravishankar, "Mechanical properties of fly ash reinforced aluminium alloy (Al6061) composites," *International Journal of Mechanical and Materials Engineering*, vol. 6, no. 1, pp. 41–45, 2011.

[9] S. Ramabalan, H. B. Michael Rajan, I. Dinaharan, and S. J. Vijay, "Experimental investigation of MRR on in situ formed AA7075/TiB2 cast composites machining by wire EDM," *International Journal of Machining and Machinability of Materials*, vol. 17, no. 3-4, p. 295, 2015.

[10] T. P. Naik, P. K. Patowari, K. G. Melese, R. S. Rana, I. Singh, and A. K. Sharma, "Process optimization of WEDM for machining of aluminum (6063)/graphite metal matrix composites," in *Advances in Engineering Design*, Lecture Notes in Mechanical Engineering, P. K. Rakesh, A. K. Sharma, and I. Singh, Eds., Springer, Singapore, 2021.

[11] K. Ishfaq, S. Anwar, M. A. Ali et al., "Optimization of WEDM for precise machining of novel developed Al6061-7.5% SiC squeeze-casted composite," *International Journal of Advanced Manufacturing Technology*, vol. 111, no. 7-8, pp. 2031–2049, 2020.

[12] V. K. Lindroos and M. J. Talvitie, "Recent advances in metal matrix composites," *Journal of Materials Processing Technology*, vol. 53, no. 1-2, pp. 273–284, 1995.

[13] P. Sivaprakasam, P. Hariharan, and G. Elias, "Experimental investigations on magnetic field-assisted micro-electric discharge machining of Inconel alloy," *International Journal of Ambient Energy*, pp. 1–8, 2020.

[14] P. Sivaprakasam, J. Udaya Prakash, and P. Hariharan, "Enhancement of material removal rate in magnetic field-assisted micro electric discharge machining of aluminium matrix composites," *International Journal of Ambient Energy*, pp. 1–6, 2019.

[15] P. Sivaprakasam and P. Hariharan, "Surface characteristics of nano powder mixed micro-wire electrical discharge machining on Inconel alloy," *Materials Today: Proceeding*, vol. 38, no. 2, pp. 494–498, 2021.

[16] G. Sozhamannan, S. Balasivanandha Prabu, and V. S. K. Venkatajalapathy, "Effect of processing parameters on metal matrix composites: stir casting process," *Journal of Surface Engineered Materials and Advanced Technology 2*, vol. 2, no. 1, pp. 11–15, 2012.

[17] J. Udaya Prakash, S. Jebarose Juliyana, P. Pallavi, and T. V. Moorthy, "Optimization of wire EDM process parameters for machining hybrid composites (356/B4C/fly ash) using Taguchi technique," *Materials Today: Proceedings*, vol. 5, no. 2, pp. 7275–7283, 2018.

[18] K. Govindan and J. G. T. Raghuvaran, "Mechanical properties and metallurgical characterization of LM25/ZrO2 composites fabricated by stir casting method," *Matéria*, vol. 24, no. 3, 2019.

[19] R. Ramanujam, P. A. Shinde, R. Kadam, A. Dey, and H. Shinde, "Estimation of optimum machining parameters and surface characterization for WEDM of AA7075/10/$Al_2O3$ (p) MMC through multi-objective optimization," *Materials Today: Proceedings*, vol. 5, no. 5, Part 2, pp. 12330–12338, 2018.

[20] B. K. Prasad, "Investigation into sliding wear performance of zinc-based alloy reinforced with SiC particles in dry and lubricated conditions," *Wear*, vol. 262, no. 3-4, pp. 262–273, 2007.

[21] A. M. Hassan, A. Alrashdan, M. T. Hayajneh, and A. T. Mayyas, "Prediction of density, porosity and hardness in aluminum-copper-based composite materials using artificial neural network," *Journal of Materials Processing Technology*, vol. 209, no. 2, pp. 894–899, 2009.

[22] S. Vijayabhaskar, T. Rajmohan, T. V. Pranay Sisir, J. V. S. Phani Abishek, D. S. Khan, and R. M. Reddy, "Review of WEDM studies on metal matrix composites," in *IOP Conf. Series: Materials Science and Engineering*, vol. 390, p. 012051, IOP Publishing, 2018.

[23] S. S. Kumar, F. Erdemir, T. Varol, S. T. Kumaran, M. Uthayakumar, and A. Canakci, "Investigation of WEDM process parameters of Al-SiC-$B_4C$ composites using response surface methodology," *International Journal of Lightweight Materials and Manufacture*, vol. 3, no. 2, pp. 127–135, 2020.

[24] S. H. Aghdeab, R. R. Shwaish, and T. M. Salman, *Effect of input parameters on MRR and EWR for tool steel AISI L2 by electric discharge machine (EDM)*, IOP Conf. Series: Materials Science and Engineering 1076 (2021) 012071, IOP Publishing, 2021.

[25] V. K. Saini, Z. A. Khan, and A. N. Siddiquee, "Advancements in non-conventional machining of aluminum metal matrix composite materials," *International Journal of Engineering Research & Technology*, vol. 1, no. 3, 2012.